

Analysis of edge effects for deformable mirrors

Javier Alda

Complutense University of Madrid
Optics Department
Faculty of Physics
Ciudad Universitaria s/n
28040 Madrid, Spain

Glenn D. Boreman, MEMBER SPIE

University of Central Florida
Department of Electrical Engineering
Center for Research in Electro-Optics and
Lasers
Orlando, Florida 32816

Abstract. Edge effects for small deformable mirrors (DMs) with few actuators are analyzed by a matrix perturbation approach. An approximate transfer-function model is developed for spatial-frequency analysis of DMs, which includes edge effects.

Subject terms: deformable mirror; adaptive optics; transfer function; matrix optics.

Optical Engineering 31(11), 2282-2286 (November 1992).

1 Introduction

Deformable mirrors (DMs) have improved the image quality delivered by optical telescopes and corrected atmospheric perturbation effects on laser-beam propagation. Large-aperture DMs that contain many actuators are used, in conjunction with specially designed computers and signal-processing systems,¹ most frequently for high-performance applications. Harvey and Callahan^{2,3} and Moore and Lawrence⁴ developed a transfer-function model suitable for large DMs that considers the spatial-filtering effect of the mirror on the variations of the incoming wavefront. Their model assumes that edge effects are negligible.

However, when the specifications are lowered and the applications do not require state-of-the-art technology, smaller DMs with fewer actuators can be used. The reduced size increases the importance of the individual performance of each actuator and increases the effect of the (usually fixed) edge of the mirror. These effects, which differ from one mirror to the next, can be included in a transfer-function analysis of the problem.

2 Derivation of System Matrix

In a one-dimensional model, which can be extended to the two-dimensional and separable case, the resulting surface of the mirror ω_m that compensates for the incoming wavefront ω is given by

$$\omega_m(x_i) = \sum_{j=1}^J m_j(x_i) a_j, \quad (1)$$

where a_j is the actuator driving input and $m_j(x_i)$ are the J influence functions, one for each actuator, measured at the points x_i where the wavefront is sensed. This expression can be written in matrix form because the phase front is sampled at discrete locations. Equation (1) becomes

$$\omega_m = \mathbf{M} \mathbf{a}, \quad (2)$$

where ω_m is a column vector with I elements corresponding to the sampled topography of the mirror and \mathbf{M} is the $I \times J$ matrix that defines the different influence functions, which are usually assumed to be shift invariant. These influence functions are represented in a sampled fashion along the J columns of the matrix \mathbf{M} . Finally, \mathbf{a} is the column vector whose elements are the driving signal for each actuator.

Paper 20111 received Nov. 27, 1991; revised manuscript received March 21, 1992; accepted for publication March 21, 1992.
©1992 Society of Photo-Optical Instrumentation Engineers. 0091-3286/92/\$2.00.

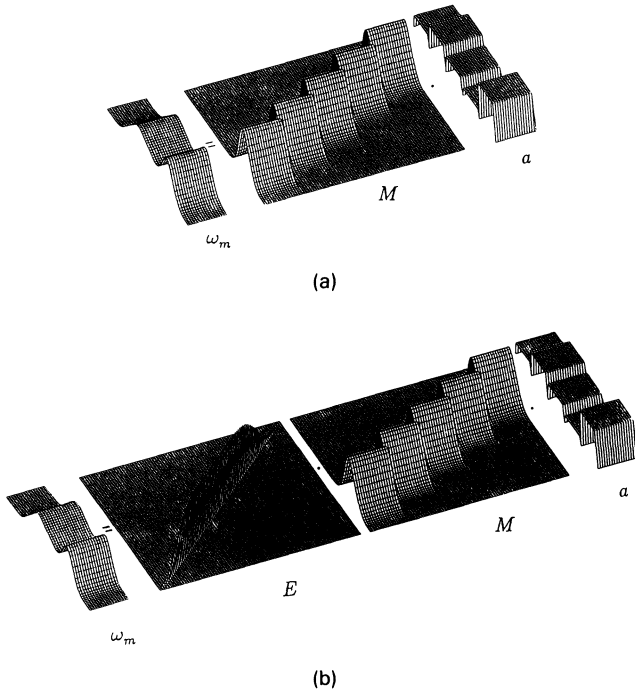


Fig. 1 (a) Graphic representation of the matrix equation $\omega_m = \mathbf{M}\mathbf{a}$ for a one-dimensional mirror with five actuators. The column vector ω_m representing the mirror profile is obtained by multiplying the actuators' driving signal \mathbf{a} by the influence function for each actuator m represented along the columns of the matrix \mathbf{M} . The dimension of the column vector \mathbf{a} (number of actuators) is smaller than the dimension of the column vector ω_m (number of sampled points). The element (0,0) is located in the lower left corner of the matrix. (b) Graphic representation of the matrix equation $\omega_m = \mathbf{E}\mathbf{M}\mathbf{a}$. The effect of the edge is introduced as a diagonal matrix where the diagonal elements are the sampled representation of the edge function $e(x)$. The element (0,0) is located in the lower left corner of the matrix.

Figure 1(a) is a graphic interpretation of this matrix equation. Using Eq. (1), the input signal for the actuators that minimizes the variance of the corrected wavefront⁵ for a given input wavefront ω , is

$$\mathbf{a} = (\mathbf{M}'\mathbf{M})^{-1}\mathbf{M}'\omega \quad (3)$$

With this driving signal, the figure of the mirror ω_m is the best compensation for the input wavefront ω at the sampled points. By substituting this solution, which minimizes the variance of the corrected wavefront, into Eq. (2), it is possible to define a system matrix \mathbf{S} that relates the input wavefront ω and the mirror profile ω_m as follows:

$$\omega_m = \mathbf{S}\omega \quad (4)$$

This transfer matrix between the input wavefront and the mirror shape is given by

$$\mathbf{S} = \mathbf{M}(\mathbf{M}'\mathbf{M})^{-1}\mathbf{M}' \quad (5)$$

We will refer to Eq. (5) as the zero-order solution because of edge effects are included. Equation (5) is the solution found by Moore and Lawrence⁴ for the case of a large number of actuators and negligible edge effects. Their solution has a clear interpretation in terms of the spatial-frequency response of the mirror.

The matrix \mathbf{S} describes the entire behavior of the mirror, assuming an optimized actuator response given by Eq. (3). Its characterization as a transfer matrix assumes that the matrix for a system with perfect wavefront correction would be a diagonal unit matrix. The deviation of the \mathbf{S} matrix from this ideal indicates to what degree the wavefront variance has been corrected. This variance of the outgoing wavefront σ^2 can be defined by using the difference between the input wavefront and the mirror figure at the sampled points. The squared modulus of the error vector $\omega - \omega_m$ yields

$$\sigma^2 = (\omega' - \omega_m')(\omega - \omega_m) \quad (6)$$

which, after using the previous relations, gives

$$\sigma^2 = \omega'(1 - \mathbf{S}')(1 - \mathbf{S})\omega = \omega'\omega - \omega'\mathbf{S}\omega \quad (7)$$

where 1 is the diagonal unit matrix. To obtain Eq. (7), we applied two useful properties of the transfer matrix: $\mathbf{S}' = \mathbf{S}$ and $\mathbf{S}^2 = \mathbf{S}$. The latter property shows that only one reflection on the mirror makes all the possible contributions for reducing the variance of the outgoing wavefront and that multiple reflections would be redundant unless shifted laterally.

When the DM is very large and there are a large number of actuators, we can make two simplifying assumptions: (1) the influence functions are equal and (2) the outer region of the mirror does not affect the general behavior of the mirror. However, when the DM is small and the edge contribution must be considered, we can define an edge function $e(x)$ that depends only on the position along the mirror and can be applied multiplicatively over all of the influence functions. Therefore, it can be introduced in the matrix formulation as

$$\omega_m(x_i) = \sum_{j=1}^J e(x_i)m_j(x_i)a_j \quad (8)$$

$$\omega_m = \mathbf{E}\mathbf{M}\mathbf{a} \quad (9)$$

Figure 1(b) is a graphic representation of Eq. (9), and Fig. 2 compares the mirror surface profiles, with and without the edge function. The edge matrix \mathbf{E} is a diagonal matrix, where the diagonal elements represent $e(x)$ sampled at the I required points. The diagonal characteristic of \mathbf{E} also implies the transposition invariance $\mathbf{E}' = \mathbf{E}$, where the superscript t denotes the transpose operation.

Using the edge function $e(x)$, it is possible to retain the previous assumptions about the influence function because the perturbative effects will appear in the \mathbf{E} matrix.

The variance σ^2 must also be minimized when the edge factor is introduced. The product $\mathbf{E}\mathbf{M}$ replaces \mathbf{M} , just as it did in passing from Eq. (2) to Eq. (9), so that the system matrix becomes

$$\mathbf{S} = \mathbf{E}\mathbf{M}(\mathbf{M}'\mathbf{E}^2\mathbf{M})^{-1}\mathbf{M}'\mathbf{E} \quad (10)$$

We will refer to Eq. (10) as the exact solution. Note that it includes the edge effect both inside and outside the matrix inversion operation. The most critical part of Eq. (10) is the inverse matrix operation $(\mathbf{M}'\mathbf{E}^2\mathbf{M})^{-1}$, whose interpretation is the interaction matrix⁶ of the orthogonalized influ-

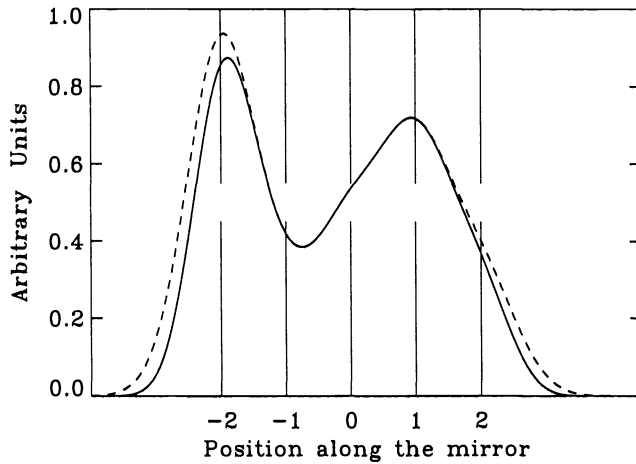


Fig. 2 Comparison of $\omega_m(x)$, the mirror's surface profile, when the edge is taken into account (solid line) or is neglected (dashed line) for a given driving signal a .

ence function affected by the edge function. This term does not have a convenient spatial-frequency representation. To gain some insight into the nature of the transfer function of the DM, including the edge effect, it is possible to decompose this factor in the following form:

$$(\mathbf{M}'\mathbf{E}^2\mathbf{M})^{-1} = (\mathbf{M}'\mathbf{M})^{-1} + \mathbf{C} \quad (11)$$

where \mathbf{C} is the difference between the situation with and without the edge effect. Although this decomposition may appear to ignore the edge in the inversion operation, the edge matrix also appears in the pre- and postmultiplicative elements of Eq. (10). Using this decomposition, the system matrix \mathbf{S} can be written as

$$\mathbf{S} = \mathbf{EM}(\mathbf{M}'\mathbf{M})^{-1} \mathbf{M}'\mathbf{E} + \mathbf{EMCM}'\mathbf{E} \quad (12)$$

The solution we refer to as the first-order solution approximates the system matrix \mathbf{S} as the first term of Eq. (12), $\mathbf{EM}(\mathbf{M}'\mathbf{M})^{-1} \mathbf{M}'\mathbf{E}$. We would expect, however, that the contribution of the edge would be somewhat overemphasized by this first-order solution because the edge matrix appears only outside the matrix inversion operation, without a compensating term inside the matrix inversion.

The first-order solution can be directly expressed using the orthogonalized functions that result from the mirror of infinite extent.⁴ It is then possible to obtain the mirror profile in the following way:

$$\omega_m(x) = [e(x)m'(x)] \star \left(\{[m'(x)e(x)] \star \omega(x)\} \text{comb}\left(\frac{x}{T}\right) \right) \quad (13)$$

where $m'(x)$ are the orthogonalized influence functions, T is the actuator spacing, and $*$ and \star represent the convolution and correlation operators, respectively. A detailed derivation of a similar expression can be found in Appendix B of Ref. 4. From Eq. (13), it is possible to realize that the edge function actually affects the individual actuator influence functions so that, even in their orthogonal form, they are no longer shifted replicas of one another. The effect of the

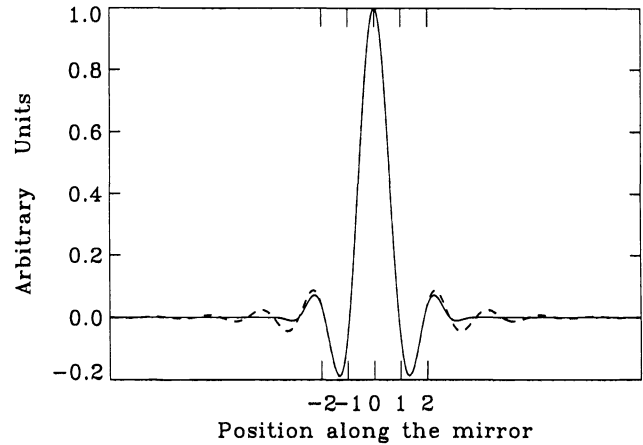


Fig. 3 Orthogonalized influence function $m'(x)$ of the mirror for an influence function $m(x)$ having Gaussian shape and a coupling factor of 37% between actuators (dashed line). Inclusion of the edge effect multiplies the orthogonalized function and produces a damping of the side lobes (solid line).

edge function on the orthogonalized influence function corresponding to the central actuator is shown in Fig. 3. The dashed line corresponds to $m'(x)$, the orthogonalized version of the Gaussian influence function. The solid line includes the effect of the edge $e(x)$ that multiplies $m'(x)$, damping the ripples. The edge function has been assumed with super-Gaussian shape. The amplitude of these ripples grows with the coupling factor between actuators. Therefore, the mirror with the edge factor acts, within this approach, like a nonedged mirror with smaller coupling between actuators.

In the Fourier transform domain;

$$\Omega_m(\xi) = [\mathcal{E}(\xi) \star \mathcal{M}'(\xi)] \{[\mathcal{M}'(\xi) \star \mathcal{E}(\xi)] \Omega(\xi) \star T\} \text{comb}(\xi T) \quad (14)$$

where Ω , \mathcal{E} , and \mathcal{M}' denote the Fourier transforms of the corresponding functions of Eq. (13). The procedure that relates the spectrum of the incoming wavefront $\Omega(\xi)$ with the spectrum of the surface of the mirror $\Omega_m(\xi)$ is a non-multiplicative procedure with a clear dependence on the edge factor. Figure 4 shows the spectrum of the orthogonalized function $\mathcal{M}'(\xi)$ (dashed line) compared with the convolution $\mathcal{M}'(\xi) \star \mathcal{E}(\xi)$ (solid line). An ideal mirror would have a rectangular spectrum with a width equal to the Nyquist frequency. Both spectra are close to this rectangular function. However, the spectrum of the nonedged mirror (dashed line) has a smoother behavior than the edged one (solid line). On the other hand, the aliasing problems that arise above the Nyquist frequency will have different importance, depending on the particular spectrum of the incoming wavefront.

3 Numerical Example

Although the first term of Eq. (12), $\mathbf{EM}(\mathbf{M}'\mathbf{M})^{-1} \mathbf{M}'\mathbf{E}$, could be represented in the spatial domain as Eq. (13) and in the spatial-frequency domain as Eq. (14), the second term of Eq. (12), $\mathbf{EMCM}'\mathbf{E}$, does not have a simple representation in either domain. To provide more insight into the contri-

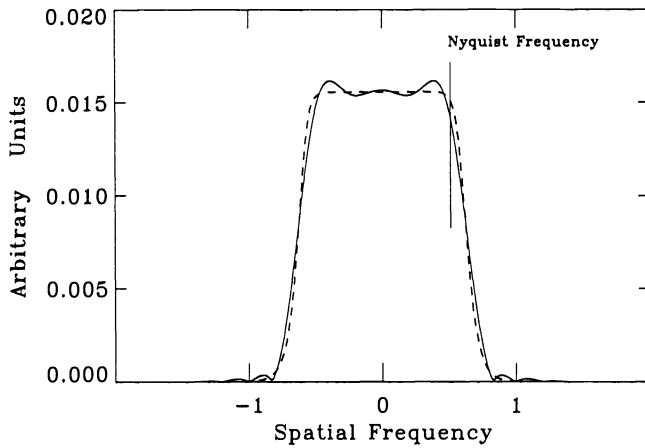


Fig. 4 Spectrum $M'(\xi)$ (dashed line) of the orthogonalized influence function compared with $M'(\xi)*E(\xi)$ (solid line), the spectrum of the product $m'(x)e(x)$ represented in Fig. 3. The Nyquist frequency is also noted.

Contributions of this term, we use a numerical calculation for a typical small mirror. Our mirror has five actuators along the studied direction. The influence functions of the individual actuators $m(x)$ are assumed equal, with Gaussian shape and coupling factor between neighboring actuators of 17%. The edge function $e(x)$ is assumed to be of super-Gaussian shape. These functions are plotted in Fig. 5. Their analytical expressions are

$$m(x) = \exp\left[-\left(\frac{x}{0.75T}\right)^2\right], \quad (15)$$

and

$$e(x) = \exp\left[-\left(\frac{x}{3T}\right)^6\right]. \quad (16)$$

Using the specific parameters of Eqs. (15) and (16), Fig. 6 presents plots of the mirror profile ω_m , calculated using Eq. (4), under the three different expressions (exact, first order, and zero order) for the transfer matrix S . In each case, ω_m is the best-fit solution for a planar input wavefront. In this example, we constrain the solution to exclude the case of zero actuator displacement to show the differences between the profiles for a simple but nontrivial case. The solid line corresponds to the exact case [Eq. (10)], where the edge effect is accounted for. The dashed line corresponds to the zero-order solution [Eq. (5)], where the edge has been ignored. The dash-dotted line represents the first-order solution, using the first term of Eq. (12), whose meaning in terms of the spatial-frequency transfer function has been found as Eq. (14). The exact solution for ω_m lies between the zero-order and first-order solutions, because the zero order completely neglects edge effects and the first order overemphasizes the edge effects. The exact solution, however, has no simple interpretation in the spatial-frequency domain because of the matrix-inversion operation required by Eq. (10). The advantage of using the first-order solution in the analysis of small DMs is that it allows an approximate spatial-frequency analysis of the edge effects.

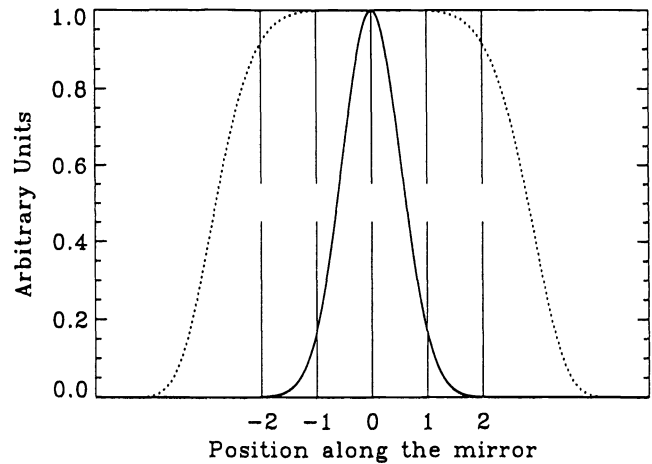


Fig. 5 Influence function $m(x)$ (solid line) and the edge function $e(x)$ (dotted line) for the case analyzed numerically. The influence function has a Gaussian shape with a coupling factor of 17%. The edge function is a super-Gaussian function (dotted line). The ticks are located at the positions of the actuators.

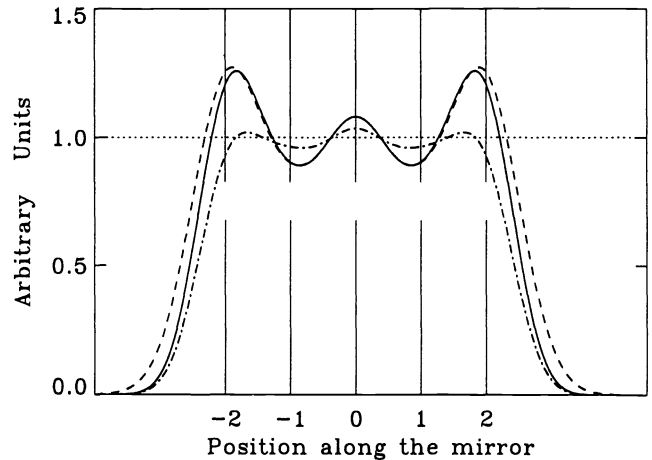


Fig. 6 Mirror surface ω_m produced in response to an input plane wave is represented in this figure according to the equation $\omega_m = S\omega$ for the case of nonzero actuator displacement. Three cases are analyzed: exact response (solid line), zero-order response (dashed line), and first-order response (dash-dotted line).

4 Conclusions

For the analysis of a small DM with few actuators, it is not possible to directly use the zero-order approach of Eq. (5) to find the spatial-frequency response because assumptions about the invariance of the influence functions and the negligible effect of the edge are violated. The exact solution of Eq. (10) has no simple interpretation in the spatial-frequency domain but can be approximated by the first term of Eq. (12). This first-order approach, while overemphasizing the effect of the edge, allows an extension of the transfer-function analysis given in Refs. 2 through 4 to the case of a DM with non-negligible edge effects.

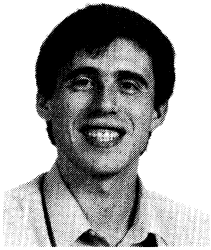
Acknowledgments

This work was performed during a stay of one of the authors (Javier Alda) at the Center for Research in Electro-Optics

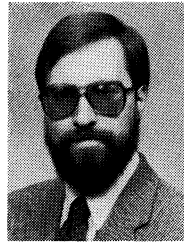
and Lasers (CREOL), University of Central Florida. The visit was supported by the Programa de Perfeccionamiento y Movilidad del Personal Investigador, BE90-140, from the Dirección General de Investigación Científica y Tecnológica (Spain), and by the Florida High Technology and Industry Council.

References

1. R. K. Tyson, *Principles of Adaptive Optics*, Academic Press, Boston, (1991).
2. J. E. Harvey and G. M. Callahan, "Wavefront error compensation capabilities of multi actuator deformable mirror," *Proc. SPIE* **141**, 50-57 (1978).
3. J. E. Harvey and G. M. Callahan, "Transfer function characterization of deformable mirrors," *J. Opt. Soc. Am.* **67**, 1367 (1977).
4. K. E. Moore and G. N. Lawrence, "Zonal model of an adaptive mirror," *Appl. Opt.* **29**, 4622-4628 (1990).
5. C. Lawson and R. Harson, *Solving Least-Square Problems*, Prentice-Hall, Englewood Cliffs, N.J. (1979).
6. R. K. Tyson, "Using the deformable mirror as a spatial filter: application to circular beams," *Appl. Opt.* **21**, 787-795 (1990).



Javier Alda received the LicSc degree in 1985 from the University of Zaragoza and the PhD degree in physics from the Complutense University of Madrid in 1988. He is currently a professor of applied optics at the University School of Optics, where he has been since 1985. He was a visiting professor during 1989 and 1991 to 1992 at the Center for Research in Electro-Optics and Lasers, University of Central Florida. His principal interest areas are laser-beam propagation and industrial inspection systems.



Glenn D. Boreman received his BS degree in optics from the University of Rochester in 1978 and his PhD degree in optical sciences from the University of Arizona in 1984. He has held visiting technical staff positions at ITT, Texas Instruments, U.S. Army Night Vision Laboratory, and McDonnell Douglas. Boreman has been at the University of Central Florida since 1984 and is currently an associate professor of electrical engineering. He is a member of OSA, IEEE, and SPIE; is past president of the Florida section of OSA; and is topical editor for *Applied Optics* in the areas of radiometry and detectors.